Nat. Hazards Earth Syst. Sci., 19, 2841–2854, 2019
https://doi.org/10.5194/nhess-19-2841-2019
© Author(s) 2019. This work is distributed under
the Creative Commons Attribution 4.0 License.

Natural Hazards and Earth System Sciences
Open Access
EGU

Analysis of spatiotemporal variations in middle-tropospheric to upper-tropospheric methane during the Wenchuan $M_S = 8.0$ earthquake by three indices

Jing Cui[1], **Xuhui Shen**[1], **Jingfa Zhang**[1], **Weiyu Ma**[2], **and Wei Chu**[1]

[1]Key Laboratory of Crustal Dynamics, Institute of Crustal Dynamics, China Earthquake Administration, Beijing 100085, China
[2]China Earthquake Networks Center, Beijing 100045, China

Correspondence: Jing Cui (jingcui_86@yahoo.com)

Received: 13 November 2018 – Discussion started: 7 January 2019
Revised: 18 September 2019 – Accepted: 28 October 2019 – Published: 17 December 2019

Abstract. This research studied the spatiotemporal variation in methane in the middle to upper troposphere during the Wenchuan earthquake (12 May 2008) using AIRS retrieval data and discussed the methane anomaly mechanism. Three indices were proposed and used for analysis. Our results show that the methane concentration increased significantly in 2008, with an average increase of 5.12×10^{-8}, compared to the average increase of 1.18×10^{-8} in the previous 5 years. The absolute local index of change of the environment (ALICE) and differential value (diff) indices can be used to identify methane concentration anomalies. The two indices showed that the methane concentration distribution before and after the earthquake broke the distribution features of the background field. As the earthquake approached, areas of high methane concentration gradually converged towards the west side of the epicenter from both ends of the Longmenshan fault zone. Moreover, a large anomalous area was centered at the epicenter 8 d before the earthquake occurred, and a trend of strengthening, weakening and strengthening appeared over time. The gradient index showed that the vertical direction obviously increased before the main earthquake and that the value was positive. The gradient value is negative during coseismic or post-seismic events. The gradient index reflects the gas emission characteristics to some extent. We also determined that the methane release was connected with the deep crust–mantle stress state, as well as micro-fracture generation and expansion. However, due to the lack of any technical means to accurately identify the source and content of methane in the atmosphere before the earthquake, an in-depth discussion has not been conducted, and further studies on this issue may be needed.

1 Introduction

The great Wenchuan $M_S = 8.0$ earthquake, on 12 May 2008, occurred in the Longmenshan fault zone in western Sichuan Province, China. Its epicenter was located at 30.95° N, 103.40° E. The extent of the earthquake and aftershock affected areas in the northeast along the Longmen Shan fault, a thrust structure along the border of the Tibetan Plateau and the western Sichuan Basin (Fig. 1). This earthquake was one of the worst continental earthquake events to have struck China in recent decades, and it killed more than 10 000 people in several cities along the western Sichuan basin. A surface rupture more than 200 km long formed along the Yingxiu–Beichuan fault. The Guanxian–Jiangyou fault was also ruptured by surface ruptures that were more than 60 km long, as indicated. The Longmenshan fault zone has a high dipping angle (more than 50–60°) near the surface and a low angle at depth (15–20 km). This listric shape favors significant strain or energy accumulation, forming large earthquakes. This earthquake was characterized by slow strain accumulation, a long recurrence interval and significant damage power. It is a new type of earthquake that deserves further study (Zhang et al., 2008).

The variation in soil gas concentration serves as a useful tool for monitoring earthquakes. Numerous field investiga-

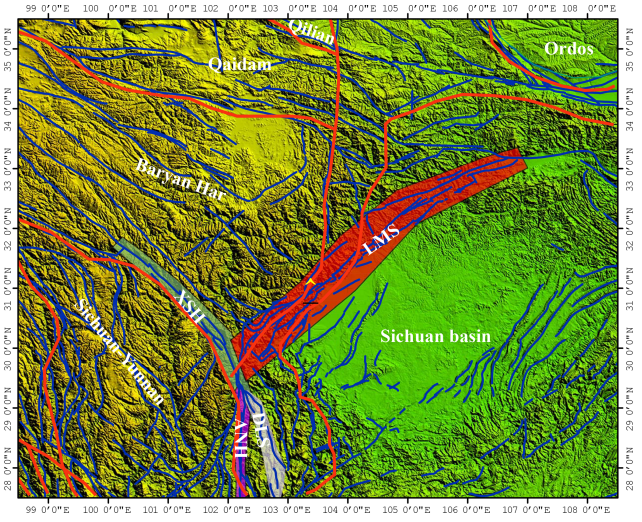

Figure 1. Map of the active faults and the location of the Wenchuan earthquake. LMS denotes the Longmenshan fault zone; XSH denotes the Xianshuihe fault zone; DLS denotes the Daliangshan fault zone; ANH denotes the Anninghe fault zone.

tions have indicated that large amounts of gases are emitted from active fault zones before, during and after great earthquakes. The increased gas emanation from the Earth's crust in the vicinity of active tectonic faults is triggered by a chain of physical processes and chemical reactions from the ground surface. This complex chain leads to geochemical, atmospheric, ionospheric and magnetospheric anomalies (Dobrovolsky et al., 1979; Pulinets and Ouzounov, 2011; Ouzounov et al., 2007). The number of pre-earthquake thermal, surface latent heat flux and outgoing longwave radiation anomalies apparently results from earthquake-related gas emission from the lithosphere (Tronin et al., 2002; Dey et al., 2004; Tronin, 2006; Ouzounov et al., 2007; Tramutoli et al., 2013). Thermal (Zhang et al., 2010), ionospheric (Lin, 2012, 2013; Zhu et al., 2010), electromagnetic (Zhang et al., 2012) and aerosol (Qin et al., 2014) anomalies were found before the Wenchuan earthquake of 12 May 2008.

As the second most important greenhouse gas after carbon dioxide (CO_2), methane (CH_4) is approximately 20 times better at warming the atmosphere than CO_2 by weight and plays an important role in atmospheric chemistry. Some people have speculated that thermal abnormalities before earthquakes are related to the release of CH_4. The CH_4 release mechanism has been investigated and results indicate strong methane emissions when friction is applied to marl-type rock (Martinelli and Plescia, 2005; Italiano et al., 2008). Yue (2013) indicated that the Wenchuan earthquake of 12 May 2008 was caused by the rapid migration and expansion of a large amount of highly pressurized and dense CH_4 gas in crustal rock masses (Yue, 2013). Sample results indicated that CH_4 was discharged from a shallow reservoir through faults or fractures caused by the earthquake (Zheng et al., 2013). This study chooses to study the spatiotemporal variations in CH_4 during the $M_s = 8.0$ Wenchuan earthquake from satellite observations.

CH_4 satellite observations have begun to be applied to seismological studies over recent years. The total column of CH_4 associated with the 12 May 2008 Wenchuan earthquake was investigated using satellite data from the AQUA Atmospheric Infrared Sounder (AIRS), and this work indicates that a large amount of CH_4 was emitted from underground into the atmosphere along the Longmenshan fault zone, from approximately 1.5 months before to 3 months after the earthquake, and the closer to the epicenter, the larger the amount of emitted gas. The peak values were found at intersection areas (Yue, 2013; Cui et al., 2017). However, the same column concentration might correspond to this distinct vertical structure. It is difficult to say whether the CH_4 anomaly is due to local sources or other atmospheric movements. The gas profile can help us understand the terrestrial emission caused by the earthquake. Recently, NASA declared that the total column values reported for CH_4 constituents are dominated by the initial guess of each and should not be used for research purposes (https://docserver.gesdisc.eosdis.nasa.gov/repository/Mission/AIRS/3.7_ScienceDataProductValidation/V6_Data_Disclaimer.pdf, last access: 30 November 2019). Previous work has shown that an AIRS for tropospheric observation can be used to carry out the study with considerable precision (Zhang et al., 2011b; Xiong et al., 2015).

Systematic observation of the vertical variation in CH_4 is scarce. The focus of this study is to examine the spatiotemporal variation in CH_4 in the middle to upper troposphere during the Wenchuan earthquake (12 May 2008) using AIRS retrieval data and to discuss the mechanism of the methane anomaly. Three indices were proposed and used for analysis: the absolute local index of change of the environment (ALICE) was used for anomaly detection, the vertical concentration gradient (gradient) was proposed for studying the vertical variation, and the successive differential value (diff) was chosen for showing the time variation. These three indices analyzed the spatial and temporal distribution of CH_4 before and after the earthquake from horizontal scales, vertical scales and timescales, helping us understand lithospheric and atmospheric interactions during seismic activity.

2 Data and methods

The version 6 and level 3 standard gridded product of 8 d CH_4 volume-mixing ratios in a descending model (local nighttime), with $1° \times 1°$ of spatial resolution, were obtained from the NASA Goddard Earth Sciences Data and Information Services Center (DISC) (http://disc.gsfc.nasa.gov/AIRS/index.shtml/, last access: 30 November 2019). The peak sensitivity of the AIRS to methane retrieval occurs at 300 hPa, and the channels near 7.6 µm are most sensitive to the mid-

dle to upper troposphere (Xiong et al., 2015). Therefore, the volume mixing ratio of the middle troposphere (400 hPa, approximately 5 km), the upper middle troposphere (300 hPa, approximately 7 km) and the upper troposphere (200 hPa, approximately 11 km) in the descending orbit data was used.

To extract the methane spatiotemporal anomalies before and after the earthquake, three parameters were applied: the absolute local index of change of the environment (ALICE) (Tramutoli, 1998; Cui et al., 2017), the vertical concentration gradient (gradient) and the successive differential (diff), all carried out on the basis of eliminating the multiyear background. The background field can partially remove the influence of natural sources such as seasonal changes and surface vegetation, effectively capturing emergency information such as earthquakes, reducing "non-seismic anomalies" to a certain extent, providing criteria for the extraction of seismic anomalies and reducing the misjudgment and leakage of seismic anomalies. It was calculated by Eq. (1):

$$G_{\mathrm{ref}}(x, y, t, l) = \sum_{i=1}^{N} G_i(x, y, t, l)/N, \quad (1)$$

$$\sigma(x, y, t, l) = \sqrt{\sum_{i=1}^{N} \left[G_i(x, y, t, l) - G_{\mathrm{ref}}(x, y, t, l)\right]^2/(N-1)}, \quad (2)$$

where $G_i(x, y, t, l)$ means the gas value in the l layer of the atmospheric pressure, measured at time t, corresponding to a location at (centered on) the coordinates (x, y); $G_{\mathrm{ref}}(x, y, t, l)$ means the reference fields for the study area, defined as a time average gas value; $\sigma(x, y, t, l)$ is the standard deviation of historical records collected under the temporal constraint. For this study, N was defined as 5 years, from 2003 to 2007; t is the time of the measurement acquisition with $t \in \tau$, where τ defines the homogeneous domain of the satellite imagery collected in the same time slot of the day and period (month) of the year; and l was defined as three layers (400 hPa, 300 and 200 hPa).

The absolute local index of change of the environment (ALICE) is calculated by Eq. (3) (Tramutoli, 1998; Cui et al., 2017):

$$\mathrm{ALICE}(x, y, t, l) = \left[G(x, y, t, l) - G_{\mathrm{ref}}(x, y, t, l)/\sigma(x, y, t, l)\right]. \quad (3)$$

The vertical concentration gradient (gradient) is used to characterize the vertical variation in gas and is calculated by Eqs. (4) to (7):

$$\mathrm{gradient}(x, y, t) = \left[G(x, y, t, \Delta l) - G_{\mathrm{ref}}(x, y, t, \Delta l)\right]/\sigma(x, y, t, \Delta l), \quad (4)$$

$$G(x, y, t, \Delta l) = G(x, y, t, l) - G(x, y, t, l+1), \quad (5)$$

$$G_{\mathrm{ref}}(x, y, t, \Delta l) = \sum_{i=1}^{N} G_i(x, y, t, \Delta l)/N, \quad (6)$$

$$\sigma(x, y, t, \Delta l) = \sqrt{\sum_{i=1}^{N} \left[G_i(x, y, t, \Delta l) - G_{\mathrm{ref}}(x, y, t, \Delta l)\right]^2/(N-1)}, \quad (7)$$

where gradient (x, y, t, l) stands for vertical concentration gradient value at level l, measured at time t, corresponding to a location at (centered on) the coordinates (x, y); $G(x, y, t, \Delta l)$ means the vertical difference of adjacent layers; $G_{\mathrm{ref}}(x, y, t, \Delta l)$ means the reference fields of the vertical difference for the study area, defined as a time average gas value; $\sigma(x, y, t, \Delta l)$ is the standard deviation of historical records collected under the temporal constraint; and l was defined as three layers (400, 300 and 200 hPa).

Successive differential value (diff) refers to the difference of the adjacent time gas value and was calculated by Eqs. (8) to (11):

$$\mathrm{diff}(x, y, \Delta t, l) = \left[G(x, y, \Delta t, l) - G_{\mathrm{ref}}(x, y, \Delta t, l)\right]/\sigma(x, y, \Delta t, l), \quad (8)$$

$$G(x, y, \Delta t, l) = G(x, y, t+1, l) - G(x, y, t, l), \quad (9)$$

$$G_{\mathrm{ref}}(x, y, \Delta t, l) = \sum_{i=1}^{N} G_i(x, y, \Delta t, l)/N, \quad (10)$$

$$\sigma(x, y, \Delta t, l) = \sqrt{\sum_{i=1}^{N} \left[G_i(x, y, \Delta t, l) - G_{ref}(x, y, \Delta t, l)\right]^2/(N-1)}. \quad (11)$$

3 Results

3.1 Reference field

The 8 d average background field at different CH_4 heights in the study area was obtained and is shown in Figs. 2–4. These figures show that the CH_4 concentration in the study area decreased significantly from the middle troposphere to the upper troposphere, and the average methane concentrations (from 9 March to 15 August 2008) in each stratum were 1.794, 1.775 and 1.762 ppm for the middle, upper middle and upper troposphere, respectively. This indicates that the middle troposphere is significantly affected by terrestrial emission sources.

The distribution of CH_4 has obvious seasonal characteristics, and the seasonal cycles at different heights are similar. The CH_4 mixing ratio has a weak high value during March and then decreases during April–May. It starts to increase in June and stays high during July and August, especially over the Sichuan basin. The relatively high values at different times are mostly located at a structural confluence or at tectonic plate boundaries except for late July and August. Earth gas emissions may be the main cause of the high long-term values at that location (http://www.climatechange2013.org/images/report/P36Doc3_WGI-12_Approved-SPM.pdf, last access: 4 December 2019). Why does the CH_4 begin to increase in early summer? Studies have shown CH_4 emissions significantly correlate with temperature. When the temperature is $< 15°$, the Earth seldom produces CH_4, and when the temperature reaches 35°, CH_4 production can be many times higher than at 25° (Kazuyuki and Katsuyuki, 1990; Thomas et al., 1996; Holzapfel-Pschorn et al., 1986; Saarnio et al., 2010; Saarnio and Silvola, 1999). Therefore, the CH_4 concentration in the troposphere is higher during July and August. The

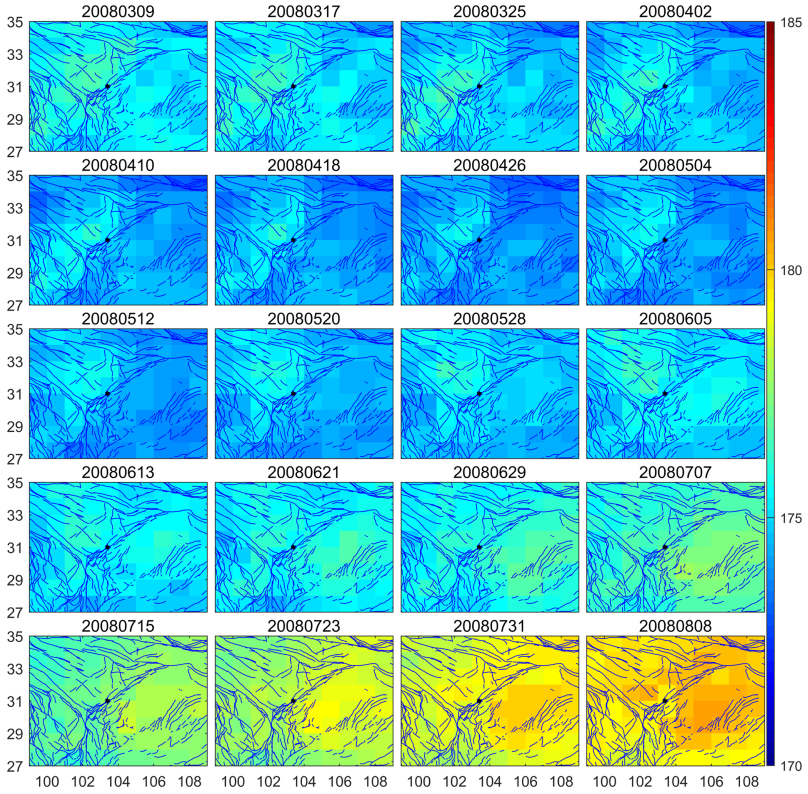

Figure 2. The 5-year (2003 to 2007) average distribution of 8 d nighttime CH_4 volume mixing ratios at 200 hPa.

CH_4 rice paddy emission, local emissions (such as from gas leakage or energy use) and transport (such as the meridional and zonal advection, convection from the lower troposphere, or stratosphere–troposphere exchange) also increase in early summer (Xiong et al., 2010).

The results of the background field analysis show that the CH_4 concentration is greatly influenced by the season, structure and underlying surface, and they present a typical spatial and temporal distribution of methane in southwestern China (Zhang et al., 2011b). Gas emanates from the Earth's crust continuously, even without earthquakes.

3.2 Anomalous gas

The three indices mentioned above have been applied to identify the spatial and temporal variation in middle-tropospheric and upper-tropospheric methane anomalies associated with the Wenchuan $M_s = 8.0$ earthquake using AIRS data.

3.2.1 ALICE index result

Figures 5–7 show that as the earthquake approached, the methane concentration near the LMS fault zone gradually increased and the range gradually expanded. High values began to appear in the northern section of the LMS fault zone on 25 March and began to increase in large areas on 4 May, showing a significant north–south distribution through the LMS fault zone. From 12 to 19 May, the high value decreased near the epicenter but remained in large parts of the study area and persisted in large areas after the earthquake. From 7 July, the northern section of the LMS fault zone again showed high accumulation. From 23 July to 7 August, the high-value zone reached the maximum, and all along the LMS fault zone it showed a NE distribution. Then the high-value areas began to weaken on 8 August. This circle was probably caused by the big aftershocks on 24 July and 1 August.

3.2.2 Vertical concentration gradient index result

The vertical concentration gradient stands for the vertical rate of change. Figures 8 and 9 show the value changing obviously at the Bayan Har block and plate boundary. The highest values appeared at the Bayan Har block, the XSH, ANH and DLS faults and lasted until 12 May before the earthquake. The values were positive before 12 May. They weaken and even turn negative after 12 May, especially during 23 July to 7 August. The overall shape is still closely related to the fault and basin edge. We will discusses this later.

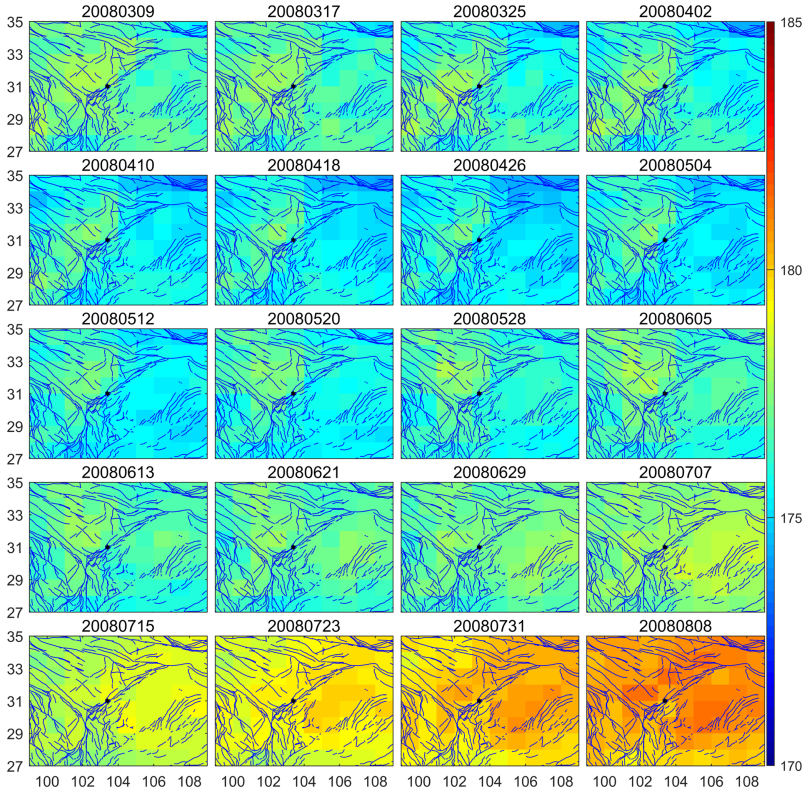

Figure 3. The 5-year (2003 to 2007) average distribution of 8 d nighttime CH_4 VMR at 300 hPa.

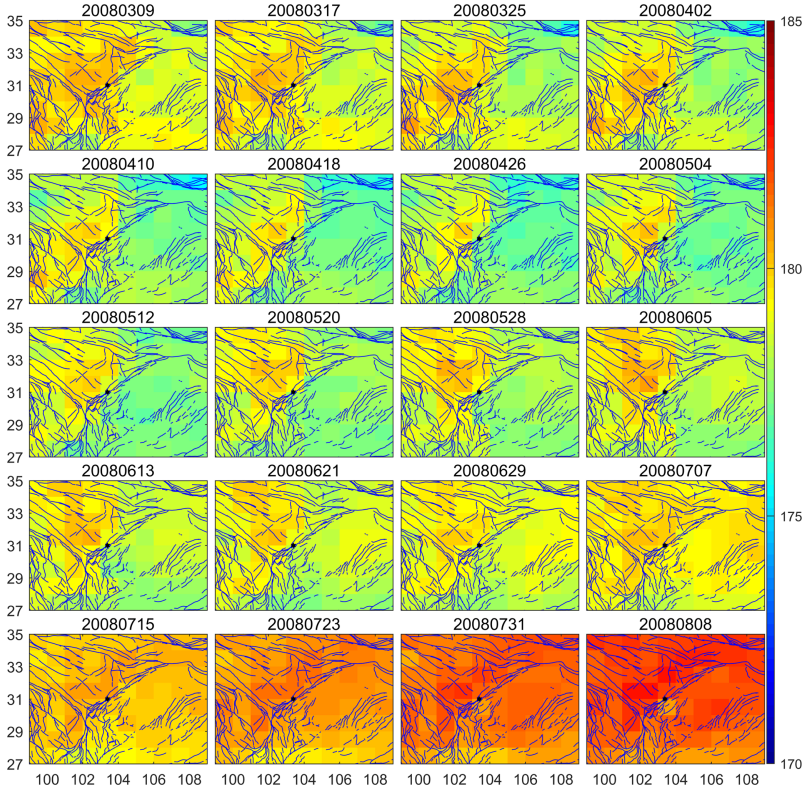

Figure 4. The 5-year (2003 to 2007) average distribution of 8 d nighttime CH_4 VMR at 400 hPa.

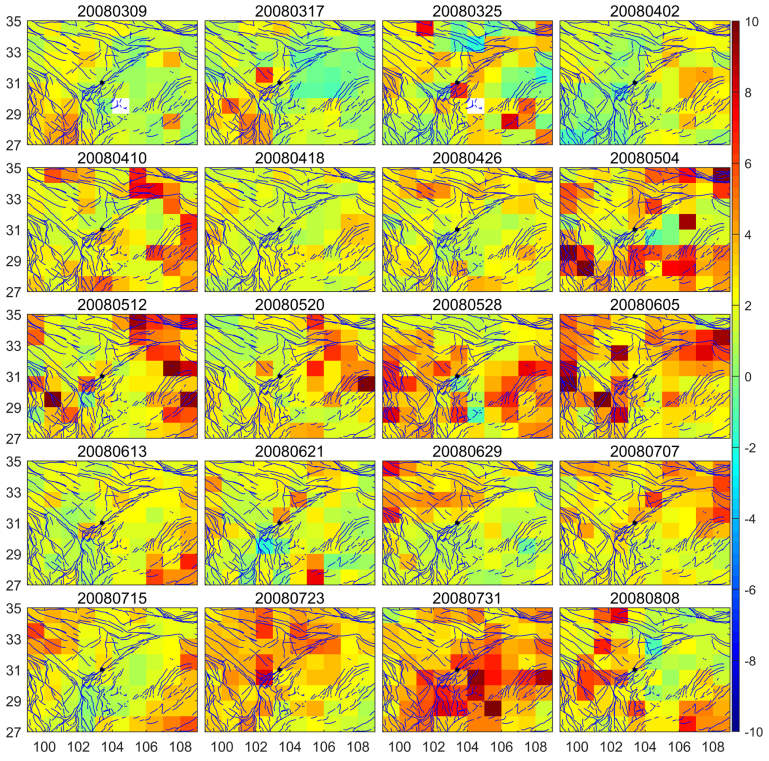

Figure 5. ALICE index of 8 d CH_4 VMR at 200 hPa.

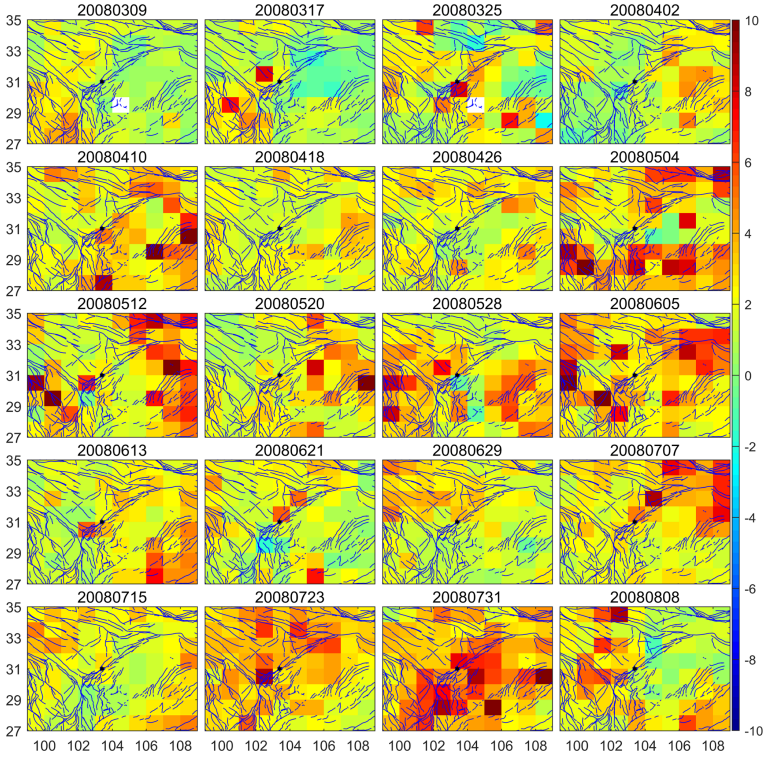

Figure 6. ALICE index of 8 d CH_4 VMR at 300 hPa.

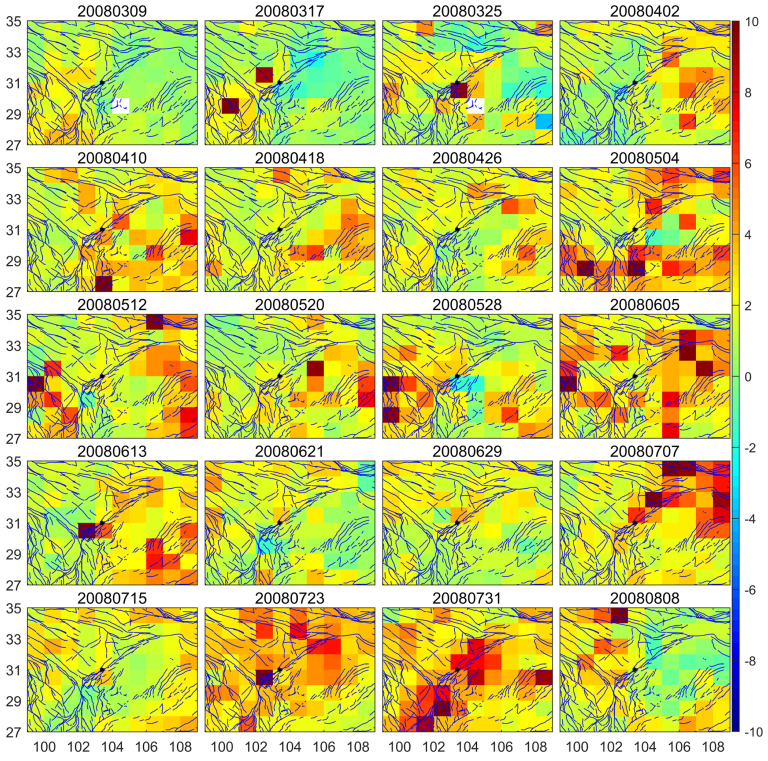

Figure 7. ALICE index of 8 d CH_4 VMR at 400 hPa.

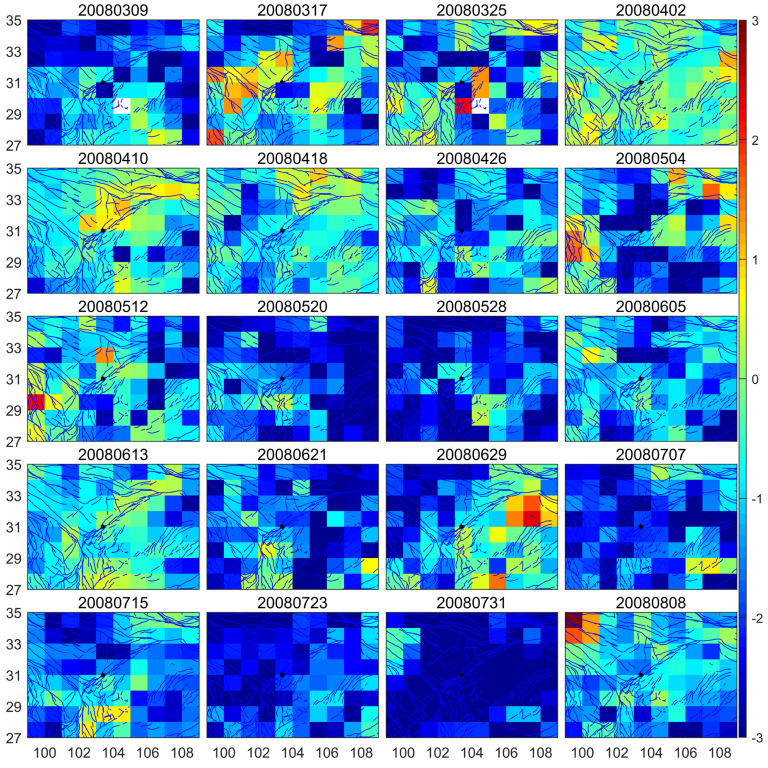

Figure 8. Gradient of 400 to 300 hPa.

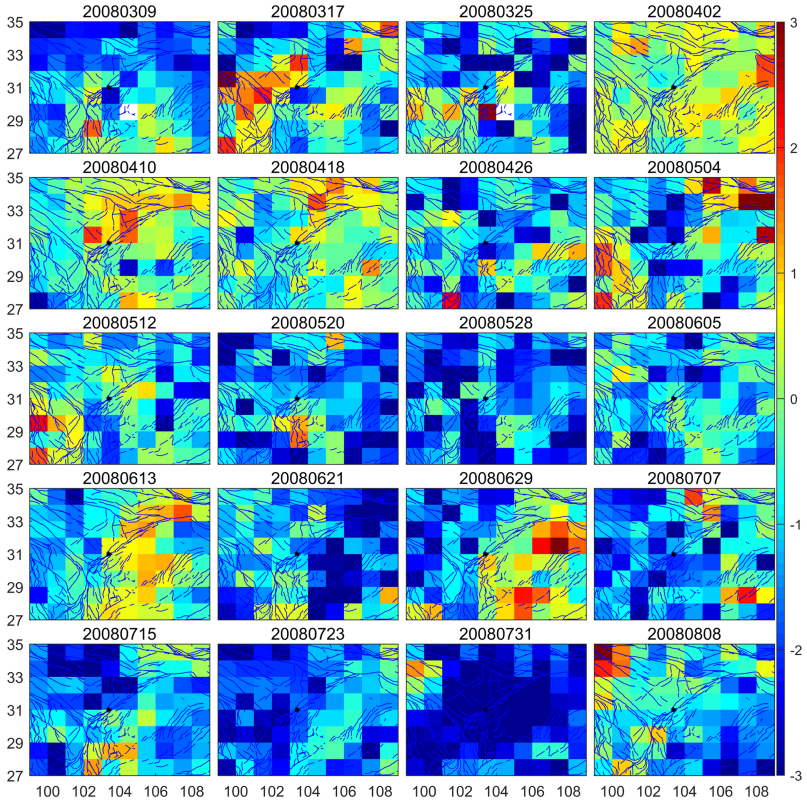

Figure 9. Gradient of 300 to 200 hPa.

3.2.3 Successive differential value

The trend of the reflected gas concentration over time was reflected by the difference change, and the result of 20080317 represented the difference between 17 and 09 March. The places with rapid changes mainly occur at plate boundaries and tectonic intersections. Figure 10 shows that the LMS fault zone began to show an abnormally high value on 25 March and then the high-value area gradually increased. On 10 April, high values appeared at the Bayan Har block, the XSH, ANH and DLS faults, and lasted until 12 May before the earthquake. The value of the entire LMS fault zone was high during 12 May. The next cycle began on 7 July, when high values first appeared in the northern section of the LMS fault zone, followed by all four LMS, XSH, ANH and DLS fault zones on 23 July. Two large aftershocks were reported on 24 July and 1 August.

4 Discussion

Background field analysis can help us understand the gas distribution in the study area and has a certain reference role for the extraction and analysis of late abnormal changes. We have found that the CH_4 concentration is greatly influenced by season, structure and underlying surface and presents a typical spatial and temporal distribution in southwestern China. Comparing our work with that of the GPS velocity field, the high-value area of the background field corresponds to the area of high GPS velocity (Wu et al., 2015). Long-term stress accumulation causes deep-Earth gases to be expelled along fissures or structural weaknesses (Wang et al., 2017).

Three indices have been used to see if anomalous CH_4 could be identified. The CH_4 spatial variations were most likely caused by geological processes and/or the action of crustal stress in the lithosphere resulting in the Wenchuan earthquake. A large amount of CH_4 was emitted from underground into the atmosphere along plate boundaries and tectonic belts from approximately 1.5 months before to 3 months after the earthquake, and the closer to the epicenter, the larger the amount of emitted gas. A large anomalous area occurs centered at the epicenter 8 d before the earthquake. A crucial question in this field of research refers to how we can link an individual precursor with a distinctive stage of the earthquake preparation.

The generation of such a seismic anomaly requires physical and chemical transformations that occur in a spatially extended preparation (activation) zone of an impending earthquake. Earthquakes, in general, exhibit complex correlations in time, space and magnitude. It is widely accepted that the observed earthquake scaling laws indicate the existence of phenomena closely associated with the proximity of the system to a critical point (Varotsos et al., 2019). Therefore, such

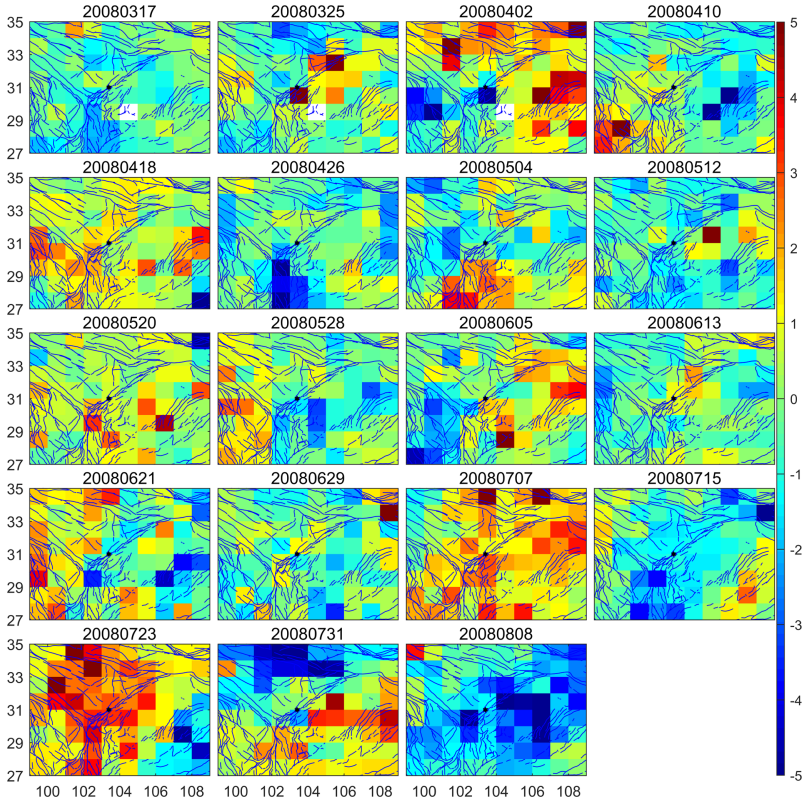

Figure 10. Distribution of the successive differential value at 300 hPa.

a requirement is satisfied during the appearance of the "critical window", i.e., the epoch during which the short-range correlations have evolved to long-range ones in an extended area, where the "critical radius R" is given by the empirical relation $\log R \approx 0.5M$ and where M is the earthquake magnitude (Bowman et al., 1998). Note that, based on the recently introduced concept of "natural time" by Varotsos et al. (2011), it has been shown that the foreshock seismic activity that occurs in the region around the epicenter of the upcoming significant shock from a few days to 1 week before the main shock occurrence behaves as critical phenomenon.

Therefore, the hypothesis that the large anomaly in methane 8 d before the earthquake occurred corresponds to the critical point window of the earthquake preparation process cannot be excluded. Accumulated experimental evidence supports the aforementioned hypothesis as follows.

The earthquake preparatory process has various facets that correspondingly reflect different precursors. Importantly, precursors emerge during the same period, from a few days up to one week before the main shock occurrence, while they behave as critical phenomena as well. Characteristically, such as precursors are (i) ultra-low-frequency magnetic field variations recorded by ground-based magnetic observatories before significant earthquakes (e.g., Contoyiannis et al., 2016; Potirakis et al., 2018) and (ii) megahertz-fracture-induced megahertz electromagnetic anomalies(Eftaxias et al., 2018). The generation of such a seismic anomaly also requires physical and chemical transformations which occur in a spatially extended preparation (activation) zone of an impending earthquake.

Characteristic precursors are the short-lived seismo-ionospheric EM precursors and EM anomalies rooted in pre-seismic lithosphere–atmosphere–ionosphere coupling (Pulinets et al., 2003; Pulinets and Boyarchuk, 2004). Pulinets et al. (2003) provide strong evidence for the occurrence of ionospheric precursors well before the main shock: ionospheric precursors within 5 d before the seismic shock were registered in 73 % of the cases for earthquakes with a magnitude of 5 and in 100 % of the cases for earthquakes with a magnitude of 6.

To further verify that the increase in CH_4 concentration is related to earthquakes, we compared and analyzed the variation in overall methane concentration and anomaly index in the study area for non-seismic years (Figs. 11 and 12, there was no large earthquake during 2003 to 2007). Compared with 2003–2007 (Fig. 11), the CH_4 concentration increased significantly in 2008, with an average increase of 5.12×10^{-8}, compared with the average increase of 1.18×10^{-8} in the past 5 years (Fig. 11), especially between 25 March and 21 June. The results from the past 5 years showed that the concentration of CH_4 increased significantly due to seasonal influence from 21 June, showing a rapid increase in the slope

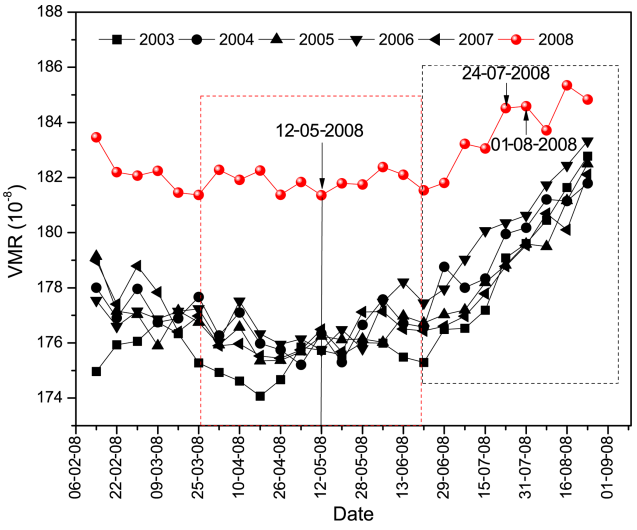

Figure 11. Comparison of the average CH_4 VMR in the study area from 2003 to 2008 (300 hPa).

Table 1. Linear fitting between 21 June and 1 September for different years.

Year	Linear equation	R square
2003	$y = 0.9272x + 174.15$	0.9788
2004	$y = 0.6044x + 176.53$	0.9051
2005	$y = 0.6916x + 175.51$	0.9404
2006	$y = 0.715x + 176.76$	0.9847
2007	$y = 0.7058x + 175.25$	0.9484
2008	$y = 0.4387x + 181.43$	0.8066

of the curve (Table 1). Although there was a certain increase in 2008, the curve slope was relatively small (Table 1), which may be due to the large amount of CH_4 released by the aftershock earthquake. The increasing trend of CH_4 concentration caused by seasonal change weakened between 25 March and 21 June 2008.

We also compare the ALICE result with 2008 and 2007 (Figs. 12 and 13). The distribution of the ALICE index of 8 d CH_4 VMR at 300 hPa during 2007 is very different from 2008. In 2007, the index results were similar on the whole to stable features with no significant differences. The average value is almost always between -2 to 2, except for on 7 February 2007. However, the average value for 2008 is over 2 after 10 April 2008, 1 month before the earthquake. Although gaseous anomalies can be affected by climate change, weather patterns, human activity, vegetation coverage and many other factors beyond seismic activity, these effects may be local and can be eliminated by calculation with Eqs (1) to (11). Therefore, the identified anomalies of CH_4 VMR can be considered earthquake-related (Cui et al., 2017). CH_4 is an important greenhouse gas in addition to carbon dioxide, and previous work shows that the obvious anomalies of thermal infrared brightness temperature appeared on 25 April and were mainly distributed in the LMS fault zone and its southern region (Zhang et al., 2010). These results correspond well with our work.

Compared with the non-seismic years from 2003 to 2007 (no earthquake $> M_s = 5.0$), the study area before and after the Wenchuan earthquake showed a significantly increased CH_4 anomaly. It is well known that CH_4 is in a supercritical or critical state at high temperature and pressure 10–20 km below the surface and that its physical and chemical properties are relatively stable during periods of weak tectonic activity. However, this state is also very easy to break with active geological activity. For example, the sudden expansion of the volume of cracks or cavities caused by the change of tectonic stress field can easily change the internal fluid state and cause the supercritical fluid-phase transition (Liu et al., 2000). As soon as the phase transition process begins, fluid volume and fracture expansion are triggered, resulting in a large amount of fluid spilling over the surface and spreading into the atmosphere, which is then observed by ground-based instruments or satellites (Martinelli and Plescia, 2005; Italiano et al., 2008).

Before the Wenchuan earthquake, various GPS observation points and level observations showed accelerated activity of different degrees. The LMS fault activity is characterized by a transition from tensile to compressive, and acceleration occlusion occurs near the fault field. Accelerated uplift and extension of the crust appeared in the Bayan Har block (Fang et al., 2009; Jiao et al., 2008), indicating that when the main section of the LMS fault zone is still in the state of friction lock, the relatively weak Bayan Har block shows the uplift and expansion of a large number of tensile cracks under long-term tectonic stress. It is with this process that the underground fluid surges up and overflows the surface on a large scale and then spreads and rises to the upper troposphere, resulting in the high CH_4 concentration region on the western side of the LMS in Figs. 5–10 before the earthquake. Many NW fracture surfaces were found on the western side of the LMS after the Wenchuan earthquake. With the occurrence of such cracks, microcracks or pre-slip, supercritical CH_4 inside the crust can well up and overflow, resulting in increased atmospheric CH_4 concentration.

Figures 5 to 10 show that the CH_4 concentration in the inner area of the Sichuan Basin on the eastern side of the LMS fault zone is at a low level before and after the earthquake and occasionally increases temporarily. The occasional short rise may be due to CH_4 release and diffusion from the surrounding fault zone. Although there are a large number of oil and gas deposits in the sedimentary cover of the Sichuan Basin, the present tectonic activity is relatively weak, and it is difficult to produce such phenomena as rupture and expansion in the upper crust, thus large-scale release of CH_4 and other fluids will not occur.

The migration or release of underground fluids such as CH_4 is inevitably completed by other seismic processes in

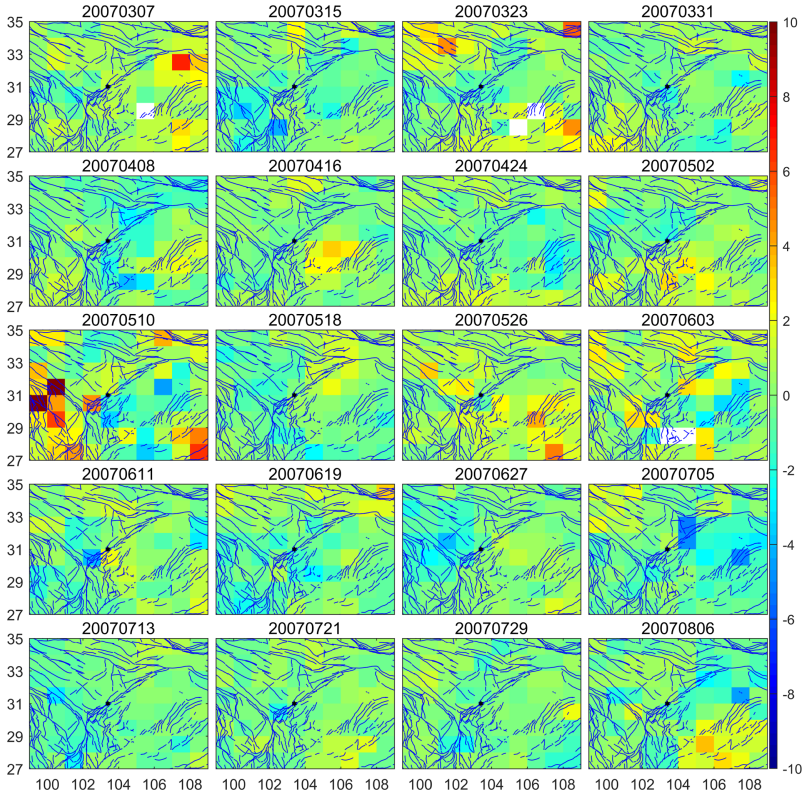

Figure 12. ALICE index of 8 d CH_4 VMR at 300 hPa during 2007.

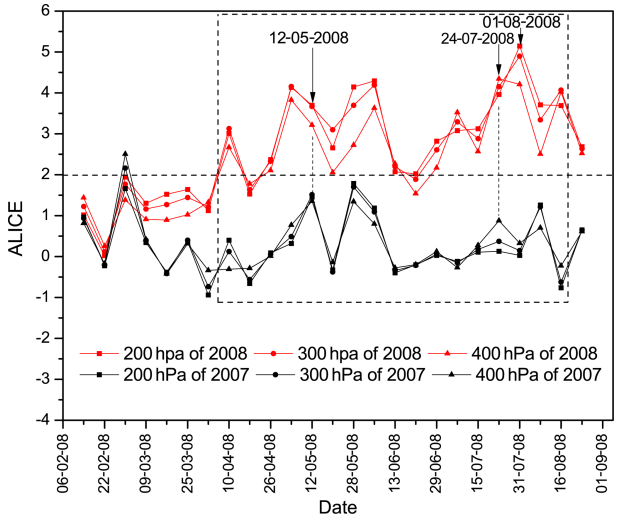

Figure 13. Comparison of the average ALICE index from 2007 and 2008.

the pre-earthquake period, which is also an important model of energy conversion and accumulation from the deep part of the crust and mantle to the shallow part of the crust. Therefore, it can be inferred that the phase transition process of underground fluids such as CH_4 was mainly completed before the earthquake, so there was an abnormal increase before the earthquake. During the earthquake and coseismic activity, the abnormal increase in fluid concentration such as CH_4 may also occur, which is mainly caused by local fluid release in the brittle layer of the upper crust (Wang et al., 2017). The range is mainly limited to the vicinity of the earthquake rupture zone, which is not on the same order of magnitude as the regional CH_4 release from the deep part. For example, the gradient shows that the values are positive before 12 May and become weak and even turn negative after 12 May (Figs. 8 and 9). The CH_4 in the upper layer may be deep gas released before the earthquake and locally released after the earthquake decreases, so the concentration of the lower layer decreases and the gradient becomes negative. The iteration of positive and negative values can also indicate geogenic emissions.

The aforementioned results seem to support the hypothesis that the observed anomaly in terms of spatiotemporal variation in methane is rooted in the stage of critical point epoch of the earthquake preparation process.

5 Conclusions

This study has examined the spatiotemporal variation in CH_4 in the middle to upper troposphere during the Wenchuan earthquake (12 May 2008), using AIRS retrieval data, and discusses the mechanism of the methane anomaly. The CH_4

concentration increased significantly in 2008, with an average increase of 5.12×10^{-8}, compared with 1.18×10^{-8} in the past 5 years. Three indices were proposed and used. The absolute local index of change of the environment (ALICE) was used for anomaly detection, the vertical concentration gradient (gradient) was used for the study of vertical variation and the successive differential value (diff) was chosen to show time variation. The three indices analyzed the spatial and temporal distribution of CH_4 before and after the earthquake from horizontal scales, vertical scales and timescales. Through this work, the following conclusions are obtained.

The background field of CH_4 is greatly influenced by season, structure and underlying surface and presents a typical spatial and temporal distribution of methane in southwestern China. Gas emanates from the earth's crust continuously, even without earthquakes.

The CH_4 concentrations in the upper and middle atmosphere before and after the Wenchuan earthquake have a certain temporal and spatial variation. The ALICE and diff indices could be used to identify the CH_4 concentration anomaly. The research results indicate that the CH_4 concentration distribution before and after the earthquake breaks the distribution features of the background field. The CH_4 concentration distribution starts from both ends and gradually gathers around the epicenter. Moreover, a large anomalous area occurs centered at the epicenter 8 d before the earthquake, and a trend of strengthening, weakening and strengthening appears over time.

The gradient method can reflect the change in gas concentration in the vertical direction. The results show that the vertical direction obviously increases before the main earthquake, and the value is positive. The gradient value is negative during coseismic or post-seismic events. It may be that the gas before the main earthquake mainly comes from deep fluid-phase transitions, whereas the coseismic or post-seismic gas may mainly come from the locally closed fluid in the brittle layer of the crust. However, due to the lack of any technical means to accurately identify the source and content of methane in the atmosphere before the earthquake, an in-depth discussion has not been conducted, and further studies on this issue may be needed. The gradient index can reflect the characteristics of gas emission to some extent.

Data availability. The data used to support the findings of this study are available from the corresponding author upon request. It is also possible to download all of the original study data from the NASA Goddard Earth Sciences Data and Information Services Center (DISC) (https://disc.gsfc.nasa.gov/datasets/AIRS3ST8_006/summary?keywords=%22AIRS%22, last access: 11 December 2019). Please click button under "data access" to access the data when logging into the website. We set the date range from 9 September 2003 to 15 August 2008. The latitude and longitude range was set to 27–35° N, 99–109° E. The descending CH_4 VMR of the methane variables has been chosen for study.

Author contributions. JC designed this study, performed most of the data analysis and wrote the paper. XS contributed to the discussions.

Competing interests. The authors declare that they have no conflict of interest.

Acknowledgements. The authors would like to thank NASA for making the AIRS dataset available. The authors wish to thank the anonymous reviewers for their constructive comments that helped improve the scholarly quality of the paper.

Financial support. This research has been supported by the National Natural Science Foundation of China (grant no. 41602223), National Key R&D Program of China (grant no. 2018YFC1503505), and the Institute of Crustal Dynamics, China Earthquake Administration (grant no. ZDJ2018-18).

Review statement. This paper was edited by Filippos Vallianatos and reviewed by two anonymous referees.

References

Bowman, D., Ouillon, G., Sammis, C., Sornette, A., and Sornette, D.: An observational test of the critical earthquake concept, J. Geophys. Res.-Solid, 103, 24359–24372, 1998.

Contoyiannis, Y., Potirakis, S., Eftaxias, K., Hayakawa, M., and Schekotov, A.: Intermittent criticality revealed in ULF magnetic fields prior to the 11 March 2011 Tohoku earthquake ($M_w = 9$), Physica A, 452, 19–28, 2016.

Cui, Y., Ouzounov, D., Hatzopoulos, N., Sun, K., Zou, Z., and Du, J.: Satellite observation of CH_4 and CO anomalies associated with the Wenchuan M_S8.0 and Lushan M_S7.0 earthquakes in China, Chem. Geol., 469, 185–191, 2017.

Dey, S., Sarkar, S., and Singh, R. P.: Anomalous changes in column water vapor after Gujarat earthquake, Adv. Space Res., 33, 274–278, 2004.

Dobrovolsky, I. P., Zubkov, S. I., and Miachkin, V. I.: Estimation of the size of earthquake preparation zones, Pure Appl. Geophys., 117, 1025–1044, 1979.

Eftaxias, K., Potirakis, S. M., and Contoyiannis, Y.: Four-Stage Model of Earthquake Generation in Terms of Fracture-Induced Electromagnetic Emissions: A Review, in: Complexity of Seismic Time Series, Elsevier, the Netherlands, 437–502, 2018.

Fang, D. U., Wen, X. Z., Zhang, P. Z., and Xi, A.: Interseismic deformation across the Longmenshan fault zone before the 2008 M8.0 Wenchuan earthquake, Chin. J. Geophys., 52, 2729–2738, 2009.

Holzapfel-Pschorn, A., Conrad, R., and Seiler, W.: Effects of vegetation on the emission of methane from submerged paddy soil, Plant Soil, 92, 223–233, 1986.

Italiano, F., Martinelli, G., and Plescia, P.: CO_2 Degassing over Seismic Areas: The Role of Mechanochemical Production at the Study Case of Central Apennines, Birkhäuser, Basel, 2008.

Jiao, Q., Yang, X., Xu, L., and Wang, B.: Preliminary Study On Motion Characteristics Of Longmenshan Fault Before And After M_S8.0 Wenchuan Earthquake, J. Geod. Geodynam., 28, 7–11, 2008.

Kazuyuki, Y. and Minami, K.: Effect of organic matter application on methane emission from some Japanese paddy fields, Soil Sci. Plant Nutr., 36, 599–610, 1990.

Lin, J. W.: Potential reasons for ionospheric anomalies immediately prior to China's Wenchuan earthquake on 12 May 2008 detected by nonlinear principal component analysis, Int. J. Appl. Earth Obs. Geoinf., 14, 178–191, 2012.

Lin, J. W.: Ionospheric anomaly at the occurring time of China's May 12, 2008, $M = 7.9$ Wenchuan Earthquake using nonlinear principal component analyses and image decoding, Egyp. J. Remote Sens. Space Sci., 16, 53–61, 2013.

Liu, W., Du, J., and Bai, L.: A review on the role of supercritical fluids in the earthquake generation, Seismol. Geol., 22, 339–444, 2000.

Martinelli, G. and Plescia, P.: Carbon dioxide and methane emissions from calcareous-marly rock under stress: experimental tests results, Ann. Geophys., 48, 167–173, 2005.

NASA Earth data: AIRS3ST8: AIRS/Aqua L3 8-day Standard Physical Retrieval (AIRS-only) $1° \times 1°$ V006, available at: https://disc.gsfc.nasa.gov/datasets/AIRS3ST8_006/summary?keywords=%22AIRS%22, last access: 11 December 2019.

Ouzounov, D., Liu, D., Kang, C., Cervone, G., Kafatos, M., and Taylor, P.: Outgoing long wave radiation variability from IR satellite data prior to major earthquakes, Tectonophysics, 431, 211–220, 2007.

Potirakis, S. M., Contoyiannis, Y., Asano, T., and Hayakawa, M.: Intermittency-induced criticality in the lower ionosphere prior to the 2016 Kumamoto earthquakes as embedded in the VLF propagation data observed at multiple stations, Tectonophysics, 722, 422–431, 2018.

Pulinets, S. and Boyarchuk, K.: Ionospheric precursors of earthquakes, Springer Science & Business Media, Berlin, 2004.

Pulinets, S. and Ouzounov, D.: Lithosphere–Atmosphere–Ionosphere Coupling (LAIC) model – An unified concept for earthquake precursors validation, J. Asian Earth Sci., 41, 371–382, 2011.

Pulinets, S., Legen'Ka, A., Gaivoronskaya, T., and Depuev, V. K.: Main phenomenological features of ionospheric precursors of strong earthquakes, J. Atmos. Sol-Terr. Phy., 65, 1337–1347, 2003.

Qin, K., Wu, L. X., Zheng, S., Bai, Y., and Lv, X.: Is there an abnormal enhancement of atmospheric aerosol before the 2008 Wenchuan earthquake?, Adv. Space Res., 54, 1029–1034, 2014.

Saarnio, S. and Silvola, J.: Effects of increased CO_2 and N on CH_4 efflux from a boreal mire: a growth chamber experiment, Oecologia, 119, 349–356, 1999.

Saarnio, S., Alm, J., Martikainen, P. J., and Silvola, J.: Effects of Raised CO_2 on Potential CH_4 Production and Oxidation in, and CH_4 Emission from, a Boreal Mire, J. Ecol., 86, 261–268, 2010.

Thomas, K. L., Benstead, J., Davies, K. L., and Lloyd, D.: Role of wetland plants in the diurnal control of CH_4 and CO_2 fluxes in peat, Soil Biol. Biochem., 28, 17–23, 1996.

Tramutoli, V.: Robust AVHRR techniques (RAT) for environmental monitoring: theory and applications, Proc. SPIE, 3496, 101–113, 1998.

Tramutoli, V., Aliano, C., Corrado, R., Filizzola, C., Genzano, N., Lisi, M., Martinelli, G., and Pergola, N.: On the possible origin of thermal infrared radiation (TIR) anomalies in earthquake-prone areas observed using robust satellite techniques (RST), Chem. Geol., 339, 157–168, 2013.

Tronin, A. A.: Remote sensing and earthquakes: A review, Phys. Chem. Earth, 31, 138–142, 2006.

Tronin, A. A., Hayakawa, M., and Molchanov, O. A.: Thermal IR satellite data application for earthquake research in Japan and China, J. Geodynam., 33, 519–534, 2002.

Varotsos, P., Sarlis, N. V., and Skordas, E. S.: Natural time analysis: the new view of time: precursory seismic electric signals, earthquakes and other complex time series, Springer Science & Business Media, Berlin, 2011.

Varotsos, P., Sarlis, N., and Skordas, E.: Natural time analysis: Important changes of the order parameter of seismicity preceding the 2011 $M9$ Tohoku earthquake in Japan, Europhys. Lett., 125, 69001, https://doi.org/10.1209/0295-5075/125/69001, 2019.

Wang, J., Xianrui, L. I., Chengchen, D. U., and Zeng, Z.: Aerial methane concentration anomaly and air temperature increase before the Wenchuan earthquake, Earth Sci. Front., 24, 331–340, 2017.

Wu, Y., Jiang, Z., Zhao, J., Liu, X., Wei, W., Liu, Q., Li, Q., Zou, Z., and Zhang, L.: Crustal deformation before the 2008 Wenchuan M S 8.0 earthquake studied using GPS data, J. Geodynam., 85, 11–23, 2015.

Xiong, X., Barnet, C. D., Zhuang, Q., Machida, T., Sweeney, C., and Patra, P. K.: Mid-upper tropospheric methane in the high Northern Hemisphere: Spaceborne observations by AIRS, aircraft measurements, and model simulations, J. Geophys. Res.-Atmos., 115, D19309, https://doi.org/10.1029/2009JD013796, 2010.

Xiong, X., Barnet, C., Maddy, E., Sweeney, C., Liu, X., Zhou, L., and Goldberg, M.: Characterization and validation of methane products from the Atmospheric Infrared Sounder (AIRS), J. Geophys. Res., 113, G00A01, https://doi.org/10.1029/2007JG000500, 2008.

Yue, Z. Q.: Cause and mechanism of highly compressed and dense methane gas mass for Wenchuan earthquake and associated rock-avalanches and surface co-seismic ruptures, Earth Sci. Front., 20, 15–20, 2013.

Zhang, P. Z., Xu, X. W., Wen, X. Z., and Ran, Y. K.: Slip rates and recurrence intervals of the Longmen Shan active fault zone,and tectonic implications for the mechanism of the May 12 Wenchuan earthquake, 2008, Sichuan, China, Chin. J. Geophys., 51, 1066–1073, 2008.

Zhang, X., Shen, X., and Miao. Y.: Electromagnetic anomalies around Wenchuan Earthquake and their relationship with earthquake preparation, Procedia Environ. Sci., 12, 693–701, 2012.

Zhang, X. Y., Bai, W. G., Zhang, P., and Wang, W. H.: Spatiotemporal variations in mid-upper tropospheric methane over China from satellite observations, Chin. Sci. Bull., 56, 3321–3327, 2011b.

Zhang, Y. S., Guo, X., Zhong, M. J., Shen, W. R., Li, W., and He, B.: Wenchuan earthquake: Brightness temperature changes from satellite infrared information, Chin. Sci. Bull., 55, 1917–1924, 2010.

Zheng, G., Xu, S., Liang, S., Shi, P., and Zhao, J.: Gas emission from the Qingzhu River after the 2008 Wenchuan Earthquake, Southwest China, Chem. Geol., 339, 187–193, 2013.

Zhu, F., Wu, Y., Lin, J., and Zhou, Y.: Temporal and spatial characteristics of VTEC anomalies before Wenchuan Ms8.0 earthquake, Geodes. Geodynam., 1, 23–28, 2010.